HYD-34

THE FLOW CHARACTERISTICS

AT AN

UNDERFLOW, SHARP-EDGED

SLUICE GATE

BY

GEORG PAJER

Translated by

EDW. F. WILSEY, ASS'T ENGR.
U. S. B. R.

THE FLOW CHARACTERISTICS
AT AN
UNDERFLOW, SHARP-EDGED
SLUICE GATE

A Translation of

Über den Strömungsvorgang

an einer unterströmten

scharfkantigen Planschütze

by

GEORG PAJER

in

Zeitschrift für angewandte

Mathematik und Mechanik
vol. 17, 1937, p. 259

Translated by

EDWARD F. WILSEY, ASS'T ENGR.

U. S. BUREAU OF RECLAMATION

Denver, Colorado,
March 15, 1938.

THE FLOW CHARACTERISTICS AT AN
UNDERFLOW, SHARP-EDGED, SIMPLE, SLUICE GATE

1. Introduction

In the earlier solutions[1,2,3] of the characteristics of two-dimensional flow through sharp-edged openings, the action of gravity was neglected, that is, the outflow velocity along the free surface of the jet was assumed constant.* Our study is based on the case shown in figure 1, and the variation of the velocity along the drop-down curve CD is analyzed in an approximate way. For two-dimensional potential flow with the aid of a hodograph method, we shall determine the pattern of the streamlines the pressure distribution on the gate $\overline{BC}$, the pressure on the bottom as well as the velocity distribution at the cross section $\overline{DC}$.

Denoting the two-dimensional motion by $z = x + iy$, the complex potential by $\phi + i\psi$ and the components of the velocity by $u_x = u \cos \theta$ and $u_y = u \sin \theta$, we have the well-known basic formula:

$$z - z_o = \int_{\phi_o + i\psi_o}^{\phi + i\psi} \frac{d(\phi + i\psi)}{u_x - iu_y} \tag{1}$$

with ψ = const., $d\psi = 0$. The equation of the streamlines can then be written after they are resolved into components, thus,

$$x - x_o = \int_{\phi_o}^{\phi} \frac{\cos \vartheta}{u} d\phi = \int_{\phi_o}^{\phi} \left(\frac{1}{u}\right)_x d\phi = \int_{\phi_o}^{\phi} v_x d\phi \tag{2}$$

---

*The superscripts refer to the references in the bibliography at the end of the paper, and the figures in parentheses refer to the numbers of the equations.

$$y - y_0 = \int_{\phi_0}^{\phi} \frac{\sin \vartheta}{u} d\phi = \int_{\phi_0}^{\phi} \left(\frac{1}{u}\right)_y d\phi = \int_{\phi_0}^{\phi} \nu_y d\phi \quad (3)$$

The quantities, $\left(\frac{1}{u}\right)_x = \nu_x$ and $\left(\frac{1}{u_y}\right) = \nu_y$

may be interpreted as the components of the reciprocal velocity,

$$\nu = \frac{1}{u_x - i u_y}$$

The graph of the reciprocal velocity of a streamline, with which we are concerned, is given by plotting vectorially from a fixed point the velocity whose magnitude is $|\frac{1}{u}|$. From (1) it follows that the graph of the reciprocal velocities of all streamlines - which we shall hereafter call the - "ν-graph" - represents a conformal map of the flow characteristics in the z-plane.

In the case of a sluice gate, the form of the ν-graph is based on the following assumptions:

I. The free surface AB in figure 1 is horizontal. The fact that the streamline $\psi = Q$ must rise gradually above the quiescent level because of the velocity of approach, u_0' is not therefore taken into consideration.

II. The line corresponding to the drop-down curve CD is replaced by a quarter ellipse (figure 3a) in the graph of the reciprocal velocity. The equation for the velocity

$$V_t = \sqrt{2g(h-y)} \quad (4)$$

is only valid at two points, C and D, on the drop-down curve. It will be shown that with this assumption, the variations between the velocities

$$|u| - |V_t|$$

computed from the velocity graph and from equation (4), are unimportant at other points of the surface of the jet for small ratios of the gate opening, a, to the head, h.

Figure 2 shows the outline of the velocity graph and the corresponding graph of ν is represented in figure (3a) by the cross-hatched area which extends to infinity. A horizontal velocity, u_o, is produced at an infinitely removed cross section A (figure 1). Point A represents the source of all streamlines. At the lower boundary of the streamlines, $\psi = 0$, the velocity has a horizontal direction and increases from u_o to

$$u_1 = 2g(h - a\alpha) \tag{5}$$

so that the corresponding point in the hodograph and in the graph of ν lies in the stretch from A to D. Point D coincides with the sink of all streamlines. The path ABCD corresponds to the upper boundary of the streamlines, $\psi = Q$. At point B, the velocity is equal to zero and atpoint C it is given by

$$u_c = \sqrt{2g(h-a)} \tag{6}$$

u_1 depends on the coefficient of contraction, α, which will be discussed later.

2. <u>The Distribution of Potential over the Graph of the Reciprocal Velocity.</u>

It must be mentioned that the actual problem consists in determining $\phi + i\psi$ as a function of the complex variable

$$\frac{1}{u_x - i u_y}$$

which is fundamentally possible on the basis of assumption II. It is known that the outer region of the ellipse shown in 3a in the ν-plane can be transferred conformally to the outer region of a unit circle in the v-plane (figure 3b) using the relation,

$$K\nu = v - \frac{\lambda^2}{v} \tag{7}$$

in which

$$v = |v| e^{i\phi}$$

is a complex variable with K and λ, constants. (K determines the scale of the graph). After separating into real and imaginary parts, we have

$$\nu_x = \frac{\cos\vartheta}{|u|} = \frac{1}{K}\left(|v| - \frac{\lambda^2}{|v|}\right)\cos\phi \qquad (8)$$

$$\nu_y = \frac{\sin\vartheta}{|u|} = \frac{1}{K}\left(|v| + \frac{\lambda^2}{|v|}\right)\sin\phi \qquad (9)$$

In the foregoing, only the fourth quadrant of both planes is considered.

If in place of v we substitute

$$v' = v^2 \;\ldots\ldots\; |v'|\, e^{i\phi'} = v^2 e^{2i\phi} \qquad (10)$$

the quarter circle $|v| = 1$ is transformed into a semicircle. The outer region of the semicircle in the lower half of the v'-plane (figure 3c) is further depicted conformally by the function

$$v'' = v' + \frac{1}{v'} \qquad (11)$$

on the entire lower half-plane (figure 4),

$$v'' = v_x'' + i\, v_y'' = |v''|\, e^{i\phi''}$$

The stretch from -2 to +2 on the v_x''-axis corresponds to the circular arc

$$|v'| = 1$$

Then

$$v'' = e^{2i\phi} + e^{-2i\phi} = 2\cos 2\phi = v_x''\,; \quad v_y'' = 0 \qquad (11a)$$

All streamlines form a family of circles which pass through the points

$$A\left(v_{0x}'' = v_0^2 + \frac{1}{v_0^2},\ v_{0y}'' = 0\right) \text{ and } D\left(v_{1x}'' = 2,\ v_{1y}'' = 0\right)$$

Their conformal mapping in parallel streamlines $\psi = 0$ to $\psi = Q$ on bands of the $(\phi + i\psi)$-plane can be accomplished by means of the function

$$\phi + i\psi = \frac{Q}{\pi}\log\left(-\frac{v_0'' - v''}{v_1'' - v''}\right) \qquad (12)$$

In this case,

$$v_1'' = 2$$

3. The Equation of the Drop-Down Curve CD.

All variables in the integrals (2) and (3) will be represented as functions of the angle ϕ. Then according to equations (11a) and (12) we have for the points on the unit circle (figure 3b)

$$\phi + i\psi = \frac{Q}{\pi}\left[\log\left(v_0'' - 2\cos 2\phi\right) - \log\left(2 - 2\cos 2\phi\right)\right] + iQ$$

$$dQ = \frac{4Q}{\pi}\left(\frac{\sin 2\phi}{v_0'' - 2\cos 2\phi} - \frac{\sin 2\phi}{2(1-\cos 2\phi)}\right)d\phi \qquad (13)$$

If the values in (8) and (13) are introduced into integral (2), we have

$$\left(|v| = 1\ ,\quad x_0 \equiv x_c = 0\right)$$

and

$$x = \frac{4Q}{\pi K}(1-\lambda^2)\left(\int_{\frac{3\pi}{2}}^{\phi}\frac{\sin\phi\cdot\cos^2\phi\, d\phi}{\frac{v_0^2}{2} - \cos^2\phi + \sin^2\phi} - \int_{\frac{3\pi}{2}}^{\phi}\frac{\sin\phi - \cos^2\phi\, d\phi}{1 - \cos^2\phi + \sin^2\phi}\right)$$

Into this equation we introduce (see equation (8))

$$Q = a\alpha u_1 = a\alpha\,\frac{K}{1-\lambda^2} \qquad (14)$$

After some short intermediate calculations we have

$$x = \frac{2a\alpha}{\pi}\left(-\int_0^{\cos\phi}\frac{\cos^2\phi\, d\cos\phi}{\frac{v_0''+2}{4} - \cos^2\phi} + \int_0^{\cos\phi}\frac{\cos^2\phi\, d\cos\phi}{1-\cos^2\phi}\right)$$

Both integrals are of the form

$$\int_0^{z}\frac{z^2\, dz}{b^2 - z^2} = \int_0^{z}\left(-1 + \frac{b^2}{b^2 - z^2}\right)dz = -z + \frac{b}{2}\log\frac{b+z}{b-z}$$

After introducing the relation

$$b = \frac{\sqrt{v_0'' + 2}}{2} = \frac{1}{2}\sqrt{v_0^2 + \frac{1}{v_0^2} + 2} = \frac{1}{2}\left(v_0 + \frac{1}{v_0}\right)$$

we obtain finally

$$x=\frac{2a\alpha}{\pi}\left[-\frac{b}{2}\log\frac{b+\cos\phi}{b-\cos\phi}+\log\left(-\cotan\frac{\phi}{2}\right)\right] \quad (15)$$

Considering equations (9), (13), and (14), equation (3) yields

$$y-a=\frac{2a\alpha}{\pi}\cdot\frac{1+\lambda^2}{1-\lambda^2}\left(\int_{-1}^{\sin\phi}\frac{\sin^2\phi \ d\sin\phi}{\frac{V_0''-2}{4}+\sin^2\phi}-\sin\phi-1\right)$$

Simplifying we have

$$c=\frac{\sqrt{V_0''-2}}{2}=\frac{1}{2}\sqrt{V_0^2+\frac{1}{V_0^2}-2}=\frac{1}{2}\left(V_0-\frac{1}{V_0}\right)=\frac{V_0^2-1}{2V_0}$$

Finally we obtain

$$y=a\left[1-\frac{2\alpha}{\pi}\cdot\frac{1+\lambda^2}{1-\lambda^2}\cdot c\cdot\left(\arctan\frac{\sin\phi}{c}+\arctan\frac{1}{c}\right)\right] \quad (16)$$

In order to evaluate the coordinates x and y, the coefficient of contraction, α, must be determined. By putting

$$\phi = 2\pi$$

we obtain from equation (16)

$$y_b=a\alpha=a\left(1-\frac{2\alpha}{\pi}\cdot\frac{1+\lambda^2}{1-\lambda^2}\cdot\frac{V_0^2-1}{2V_0}\arctan\frac{2V_0}{V_0^2-1}\right)$$

We now introduce a new angle, ε, defined thus

$$\varepsilon=\arctan\frac{2V_0}{V_0^2-1}=\operatorname{arc\,cotan}\frac{V_0^2-1}{2V_0}$$

$$0\leqq\varepsilon\leqq\frac{\pi}{2}, \text{ then } \infty\geqq V_0=\cotan\frac{\varepsilon}{2}\geqq 1$$

$$\frac{1}{\alpha}=1+\frac{2}{\pi}\frac{1+\lambda^2}{1-\lambda^2}\varepsilon\cdot\cotan\varepsilon \quad (17)$$

The coefficient of contraction

$$\alpha=\frac{y_D}{a}$$

cannot be computed as yet from this equation, because λ and ε depend on α. On account of the uniqueness of the solution, the boundary equations (5) and (6) must be taken into consideration. Equation (8) gives for cross section D with

$$\phi = 2\pi, \quad \Theta = 2\pi ;$$

$$\frac{K}{u_1} \quad \frac{K}{\sqrt{2g(h - a\alpha)}} = 1 - \lambda^2$$

If we place $\phi = 3\pi/2$ and $\theta = 3\pi/2$ in equation (9), then

$$\frac{K}{u_c} = \frac{K}{\sqrt{2g(h - a)}} = 1 + \lambda^2$$

Solving we obtain

$$\lambda^2 = \frac{\sqrt{1 - \frac{a\alpha}{h}} - \sqrt{1 - \frac{a}{h}}}{\sqrt{1 - \frac{a\alpha}{h}} + \sqrt{1 - \frac{a}{h}}} \tag{18}$$

$$K = \sqrt{2gh} \quad \frac{2\sqrt{\left(1 - \frac{a\alpha}{h}\right)\left(1 - \frac{a}{h}\right)}}{\sqrt{1 - \frac{a\alpha}{h}} + \sqrt{1 - \frac{a}{h}}} \tag{19}$$

The auxiliary angle, ε, can be determined from the equation of continuity, thus

$$\frac{u_o}{u_1} = \frac{a\alpha}{h} = \frac{1 - \lambda^2}{V_o - \frac{\lambda^2}{V_o}} = \frac{1 - \lambda^2}{\text{cotan}\frac{\varepsilon}{2} - \frac{\lambda^2}{\text{cotan}\frac{\varepsilon}{2}}}$$

$$V_o \equiv \text{cotan}\frac{\varepsilon}{2} = \frac{(1 - \lambda^2)h}{2a\alpha} + \sqrt{\frac{(1 - \lambda^2)^2 h^2}{4a^2\alpha^2} + \lambda^2} \tag{20}$$

From equations (17), (18), and (20) it is seen that theoretically α depends only on the gate opening ratio a/h. The determination of α, λ, and ε from equations (17), (18), and (20) is shown by the following numerical example:

Example: Given $h = 1.5$ meters, $a = 0.18$m; then $a/h = 0.12$. Choose $\alpha = 0.610$ and compute λ^2, and ε, and introduce these values in equation (17).

This gives $\alpha = 0.6065$. Now choose $\alpha = 0.60653$, then equation (18) gives $\lambda^2 = 0.013065$ and equation (20) yields $\varepsilon = 8°26'05''$ and therefore $v_0 = 13.5611$. Equation (17) confirms the correctness of the choice of α. After computing the constants $b = 6.8174$ and $c = 6.7437$ we can determine the coordinates of the drop-down curve (table 1). We can also check the deviations at single points of the

TABLE I

$2\pi-\phi$	90°	60°	45°	30°	15°	5°	0°
x (m)	0.0000	0.00337	0.01193	0.03101	0.07333	0.14789	∞
(a-y) (m)	0.0000	0.00938	0.02056	0.03523	0.05237	0.06459	0.07082
|w| m/sec.	5.089	5.1070	5.1285	5.1565	5.1890	5.2121	5.2238
|u| m/sec.	5.089	5.1217	5.1550	5.1891	5.2144	5.2226	5.2238
|u|-|w| m/sec.	0.000	0.0147	0.0265	0.0326	0.0254	0.0105	0.0000

streamlines from equation (4) for $\frac{3\pi}{2} < \phi < 2\pi$. After eliminating angle θ, equations (8) and (9) give a velocity corresponding to the hodograph, thus

$$|u| = \frac{K}{\sqrt{1 + \lambda^4 - 2\lambda^2 \cos 2\phi}}$$

Since the difference between the velocities u and w is insignificant,

(for $\frac{a}{h} = 0.12$, then $\frac{|u| - |w|}{|u|} = 0.63$ % max;

for $\frac{a}{h} = 0.5$, then $\frac{|u| - |w|}{|u|} = 3.8$ % max.)

it appears that the choice of function (7) for an approximate solution is valid.

In table II are given the theoretical values of α as well as the coordinates of the drop-down curve for various values of the ratio*, a/h. It is to be noticed that the streamlines for

* For $\frac{a}{h} = 0$; $a = 0.1$ m. For $a/h = 0.2 - 0.5$; $h = 1$m.

each gate opening, a, if

$$0 \leq \frac{a}{h} \leq 0.5$$

deviate from one another an insignificant amount and that the ratio

$$\frac{|u_{\Theta}| - |u_o|}{|u_{\Theta}|}$$

varies between 0 and 18 percent. From this "stability" of the drop-down curve against changing of the velocity-plane it may be concluded that the flow boundary corresponding to a rigorous solution can differ only a small amount from the curve as determined.

TABLE II

a/h		0	0.2	0.3	0.4	0.5
α		0.6110	0.6046	0.6036	0.6043	0.6066
x (m)	$\phi = 300°$	0.001925	0.00360	0.00504	0.00605	0.00655
	$\phi = 315°$	0.00678	0.01287	0.01822	0.02232	0.02473
	$\phi = 330°$	0.01754	0.03370	0.04848	0.06080	0.06960
	$\phi = 345°$	0.04130	0.08031	0.11744	0.15109	0.17947
	$\phi = 355°$	0.08308	0.16281	0.24069	0.31495	0.33932
(a-y)(m)	$\phi = 300°$	0.00521	0.01025	0.01475	0.01673	0.02071
	$\phi = 315°$	0.01140	0.02259	0.03286	0.03991	0.04798
	$\phi = 330°$	0.01945	0.03893	0.05732	0.07219	0.08744
	$\phi = 345°$	0.02883	0.05821	0.08680	0.11214	0.13838
	$\phi = 355°$	0.03549	0.07203	0.10813	0.14155	0.17689

4. Pressure Distribution along the Gate and along the Floor.

After introducing $\Theta = \frac{3\pi}{2}$

integral (3) reads

$$\int_y^h dy = h - y = -\int_{\phi}^{\phi_{\Theta}} \frac{d\phi}{|u|} \qquad (3a)$$

It is proper to express $\frac{1}{|u|}$ and ϕ as analytic functions of the variable $|v|$ (figure 3b), thus,

$$\frac{1}{|\omega|} = \frac{1}{k}\left(|v| + \frac{\lambda^2}{|v|}\right)$$

$$\phi + i\psi = \frac{Q}{\pi} \log \frac{v'' - v_0''}{v'' - 2} + iQ$$

$$= \frac{Q}{\pi}\left[\log(v_0' - v') + \log\left(\frac{1}{v_0'} - v'\right) - 2\log(1 - v')\right] + iQ \qquad (9a)$$

$$= \frac{Q}{\pi}\left[\log(v_0^2 - v^2) + \log\left(\frac{1}{v_0^2} - v^2\right) - 2\log(1 - v^2)\right] + iQ$$

For the length EC we have

$$v = -i|v| \qquad (21)$$

$$\phi = \frac{a\alpha k}{\pi(1-\lambda^2)}\left[\log(v_0^2 + |v|^2) + \log\left(\frac{1}{v_0^2} + |v|^2\right) - 2\log(1 + |v|^2)\right] \qquad (22)$$

$$d\phi = \frac{2a\alpha k}{\pi(1-\lambda^2)}\left(\frac{|v|}{v_0^2 + |v|^2} + \frac{|v|}{\frac{1}{v_0^2} + |v|^2} - \frac{2|v|}{1 + |v|^2}\right) d|v|$$

If we substitute equations (9a) and (22) in integral (3a), we have

$$h - y = \frac{2a\alpha}{\pi(1-\lambda^2)} \int_{|v|}^{\infty} \left(\frac{|v|^2 + \lambda^2}{v_0^2 + |v|^2} + \frac{|v|^2 + \lambda^2}{\frac{1}{v_0^2} + |v|^2} - 2\frac{|v|^2 + \lambda^2}{1 + |v|^2}\right) d|v|$$

$$= \frac{2a\alpha}{\pi(1-\lambda^2)} \int_{\infty}^{|v|} \left(-\frac{v_0^2 - \lambda^2}{v_0^2 + |v|^2} - \frac{\frac{1}{v_0^2} - \lambda^2}{\frac{1}{v_0^2} + |v|^2} + 2\frac{1 - \lambda^2}{1 + |v|^2}\right) d|v| \qquad (23)$$

$$= \frac{2a\alpha}{\pi(1-\lambda^2)}\left[\left(v_0 - \frac{\lambda^2}{v_0}\right) \operatorname{arccotan} \frac{|v|}{v_0} + \left(\frac{1}{v_0} - \lambda^2 v_0^2\right) \operatorname{arccotan} v_0|v|\right.$$

$$\left. - 2(1-\lambda^2) \operatorname{arccotan} |v|\right]$$

If we choose for the variable $|v|$ any value between 1 and ∞ and compute the corresponding velocity u from equation (9a), then with the aid of equation (23) every point on the gate at which this velocity occurs can be determined. In table III are given the velocities and pressures, determined from Bernoulli's equation, for several points on the gate ($h = 1.50$ m., $a = 0.18$ m.)

TABLE III

$\frac{1}{\lvert v\rvert}$	0	0.05	0.10	0.20	0.30	0.40	0.60	0.80	1.00
$-u$ (m/sec.)	0	0.2578	0.5155	1.0306	1.5448	2.0579	3.0788	4.090	5.089
$\frac{u^2}{2g}$ (m.)	0	0.0034	0.0135	0.05413	0.12164	0.2158	0.4831	0.8531	1.3200
$(h - y)$ m.	0	0.5620	0.9079	1.1351	1.2291	1.2729	1.3078	1.3180	1.3200
$\frac{p}{\gamma}$ (m.)	0	0.5586	0.8944	1.0810	1.1075	1.0571	0.8247	0.4649	0.0000

The pressure on the floor can be similarly determined. It must be observed, however, that for the streamline $\psi = 0$, equation (21) must be replaced by

$$v = |v|\, e^{2\pi i} = |v|$$

If a value of v is chosen between 1 and v_0, then the abscissa of each point at which the velocity

$$u = \frac{k}{|v| - \frac{\lambda^2}{|v|}}$$

occurs, can be computed from

$$x - x_E = \frac{a\,\alpha}{\pi(1-\lambda^2)}\Bigg[\left(v_0 - \frac{\lambda^2}{v_0}\right)\left(\log\frac{v_0 - |v|}{v_0 + |v|} - \log\frac{v_0 - v_E}{v_0 + v_E}\right)$$

$$+ \left(\frac{1}{v_0} - \lambda^2 v_0\right)\left(\log\frac{v_0|v| - 1}{v_0|v| + 1} - \log\frac{v_0 v_E - 1}{v_0 v_E + 1}\right)$$

$$- 2(1-\lambda^2)\left(\log\frac{|v| - 1}{|v| + 1} - \log\frac{v_E - 1}{v_E + 1}\right)\Bigg]$$

in which

$$v_E = \sqrt{\frac{v_E''}{2} + \sqrt{\frac{v_E''^2}{4} - 1}}\,, \quad v_E'' = \frac{6v_0'' + 4}{v_0'' + 6}$$

$$|V| = \sqrt[4]{\frac{t}{2} + \sqrt{\frac{t^2}{4} - 1}} \qquad \text{[illegible]}$$

in which

$$t = \frac{|V''|^2}{2} + \sqrt{\frac{|V''|^4}{4} - 2|V''|^2 \cos 2\phi'' + 4}$$

and

$$\cos 2\phi = \pm\sqrt{\frac{|V''|^2+4}{8} - \sqrt{\left(\frac{|V''|^2+4}{8}\right)^2 - \frac{|V''|^2}{4}\cos^2\phi''}} \qquad \text{[illegible]}$$

For determining the abscissa x_E in figure 5, the equi-potential curve EC was constructed in the following manner: On the v"-plane, the corresponding curve is represented by a circle (figure 4). The coordinates of several points of the equi-potential curve EC in the ν-plane can be computed with the aid of equations* (8) and (9). The

*Equations 24 and 25 are roots of the mapping equations (10) and (11).

determination of equi-potential lines in the Z-plane follow from the graphical evaluation of integrals analogous to equations (2) and (3), thus

$$x - x_o = -\int_{\psi_o}^{\psi'} \left(\frac{1}{u}\right)_y d\psi = -\int_{\psi_o}^{\psi} \nu_y \, d\psi$$

$$y - y_o = \int_{\psi_o}^{\psi} \left(\frac{1}{u}\right)_x d\psi = \int_{\psi_o}^{\psi} \nu_x \, d\psi$$

Curve P in figure 1 gives the total pressure against the gate (width 1 m.) for various gate openings and can be determined from the impulse principle.

$$P = \gamma\left[\frac{h'^2}{2} - \frac{a^2\alpha^2}{2} + \frac{Q'}{g}(u_o' - u_i')\right]$$

$$= \gamma\left[h'\left(\frac{h'}{2} + \frac{u_o^2}{g}\right) - a\,\alpha\left(2h - \frac{3}{2}a\,\alpha'\right)\right]$$

The values indicated by the dashed lines apply to a rigorous solution of the problem (assumptions I and II are not made). With a permissible approximation, we may put

$$\alpha' = \alpha$$

5. Comparison of Experimental Measurements with the Theoretical Results.

It may be concluded from the experiments performed in Koch's laboratory[4] and also from tests by Keutner[5] that the coefficient of contraction α is independent of the head, h. Keutner gives α as a function of the gate opening, a.

The theoretical coefficient of contraction, α, which is solely dependent on the gate opening ratio, $\frac{a}{h}$, varies between 0.6036 and 0.6110 (if a/h lies between 0 and 0.6); it is worthy of mention that it is on the average smaller than coefficient of contraction measured by Keutner, but it is larger than value of $\alpha = 0.60$ (for a = 0.18 m.; h = 1.2-1.8m.) given by Carstanjen. An agreement with this coefficient can be reached after transforming equation 18. Suppose we replace u_c and u by

$$u_c = \phi\sqrt{2g(h-a)}, \quad u_o = \sqrt{2g(h-a\alpha)}$$

where ϕ is the coefficient of velocity. These euqations agree with Keütner's velocity measurements. We obtain the expression

$$\lambda^2 = \frac{\sqrt{1-\frac{a\alpha}{h}} - \phi\sqrt{1-\frac{a}{h}}}{\sqrt{1-\frac{a\alpha}{h}} + \phi\sqrt{1-\frac{a}{h}}} \qquad (18a)$$

Equations (17) and (20) remain unchanged.

For $\frac{a}{h} = 0.12$, $\phi = 0.98$, the coefficient of contraction is found to be $\alpha = 0.6016$. This value does not differ materially from 0.60.

The coefficients of contraction, α, observed by Keutner[5] are somewhat higher for small gate openings, a. This can be attributed to the influence of the boundary flow along the gate and floor as well as the rather dull knife-edge of the gate. At greater gate openings, the water surface was severely disturbed.

By neglecting the effect of gravity[2] (the velocity along the free boundary of the jet is constant), α is found to increase rapidly with increasing values of $\frac{a}{h}$.

A comparison of the theoretical with the experimental drop-down curve as observed in Koch's laboratory is shown in figure 6 for a = 0.18 m. and h = 1.50 m. Keutner[6] sets up empirical equations for the part of the drop-down curve beginning at the knife-edge. In figure 7 several observed and theoretical curves are presented. The theoretical curves were constructed as follows: After determining the potential line $\overline{EC}$ by the method described in last section, the streamlines $\psi = \frac{Q}{4}, \frac{Q}{2}$, and $\frac{3Q}{4}$ were derived from the z'-plane by graphical integration of equations (2) and (3). The velocities at the intersections of these streamlines with the y-axis can be found from the ν-plane. For the solution the following constants were used: $\frac{a}{h} = \frac{0.1463}{0.0893} = 0.3758$, $\alpha = 0.6040$, $\lambda^2 = 0.53326$, $v_0 = 4.18343$, $v_E = 2.10163$, $u_M = 1.1077$ meters per second, $u_c = 2.1835$ meters per second.

Pressure measurements were performed in Koch's laboratory for $h = 1.5$ m., $a = 0.18$ m., and a tail-water depth of 1.15 m. (figure 9). Reducing the velocity head in table III in proportion to

$$\frac{Q_u^2}{Q^2} = \frac{Q_u^2}{2g\,a^2\alpha^2(h - a\alpha)} = \left(\frac{0.2909}{0.5703}\right)^2 = 0.2602$$

(Q_u represents the discharge measured in the tests; Q is the theoretical discharge for $h = 1.5$ m., $a = 0.18$ m., and a tail-water depth $a\alpha$), we can determine a pressure curve which agrees very well with the experimental pressure curve.

Figure 5 shows the theoretical pressure distribution along the bottom in comparison with the distribution measured in Koch's laboratory. The computed floor pressures are given in table IV.

TABLE IV

$\frac{a}{h} = \frac{0.150}{1.281} = 0.11710$; $= 0.60662$; $2 = 0.012711$; $v_0 = 13.8996$

$\frac{1}{\lvert v\rvert}$	0.1	0.2	0.3	$\frac{1}{v_E} = 0.42$	0.5
P/γ (m.)	1.2694	1.2345	1.1764	1.0755	0.9892
$(x - x_E)$ (m.)	-0.6385	-0.1945	-0.0744	0.0000	0.0347

$\frac{1}{\lvert v\rvert}$	0.6	0.8	0.9	0.95	0.98	1.0
P/γ (m.)	0.8596	0.5264	0.3228	0.2097	0.1393	0.0910
$(x - x_E)$ (m.)	0.07135	0.1441	0.1947	0.2398	0.2966	oo

Upstream from the gate the experimental and theoretical curves agree well. Below the gate the experimental curve lies higher on account of the vortices which occur.

The comparison of the theoretical and experimental curves is not unsatisfactory and shows that the use of the potential theory is justifiable for solving the problem presented in this paper.

1 Betz, A. and Petersohn, E: Anwendung der Theorie der freien Strahlen (Use of the Theory of Free Jets); Ingenieur - Archiv, 1932, p. 190.

2 Mueller, H.: Rechnerische Ermittlung der Strömungsvorgänge an scharfkantigen Planschützen (Calculation of the Flow Phenomena at Sharp-Edged Sluice Gates); Wasserkraft und Wasserwirtschaft, vol. 30, 1935, p. 281.

3 Mises, R. v.: Berechnung von Ausfluss - und Überfallzahlen Calculation of Orifice and Weir Coefficients) Zeitschrift des Vereines Deutscher Ingenieur, vol. 61, 1917, p. 447.

4 Koch, A. and Carstanjen, M.: Von der Bewegung des Wassers und dabei auftretenden Kräften (On the Motion of Water and the Forces Entering Therein); Berlin, 1926.

5 Keutner, C.: Wasserabführungsver-mögen und scharfkantigen und abgerundeten Planschützen (Discharge Characteristics of Sharp-Edged and Rounded Slide Gates); Die Bautechnik, vol. 10, 1932, pp. 266 and 303.

6 Keutner, C.: Die Strömungsvorgänge an unterströmten Schütztafeln mit scharfen und abgerundeten Unterkanten (Flow Phenomena at Underflow Sluice Gates with Sharp and Rounded Lower Edges); Wasserkraft und Wasserwirtschaft vol. 75, 1935, pp. 5 and 16.

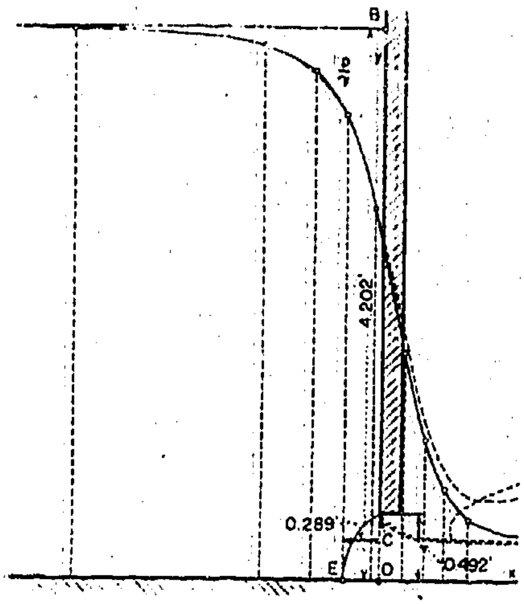

FIGURE 5

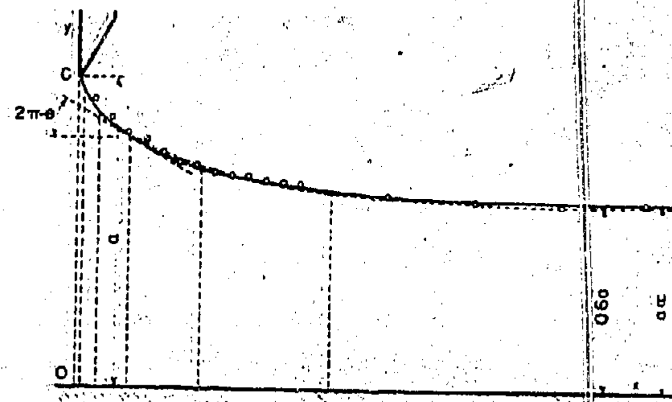

FIGURE 6

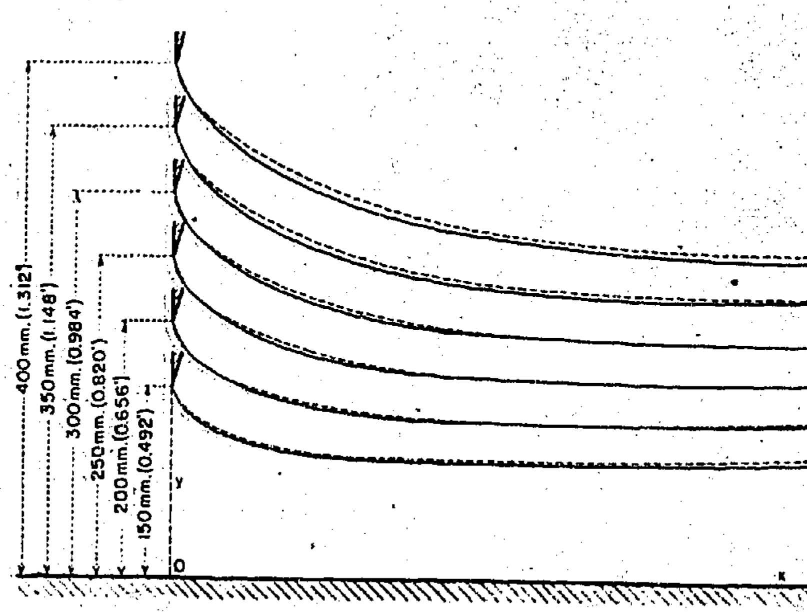

FIGURE 7

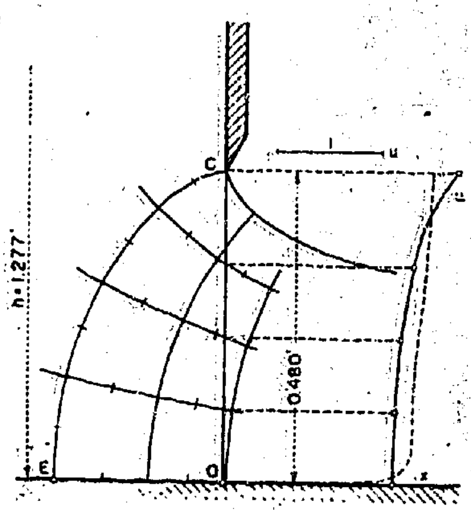

FIGURE 8

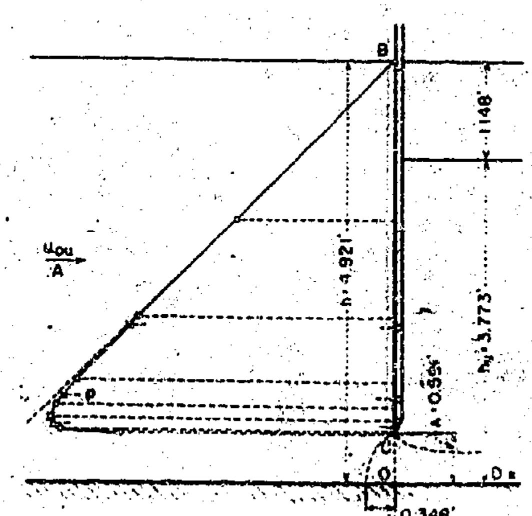

FIGURE 9

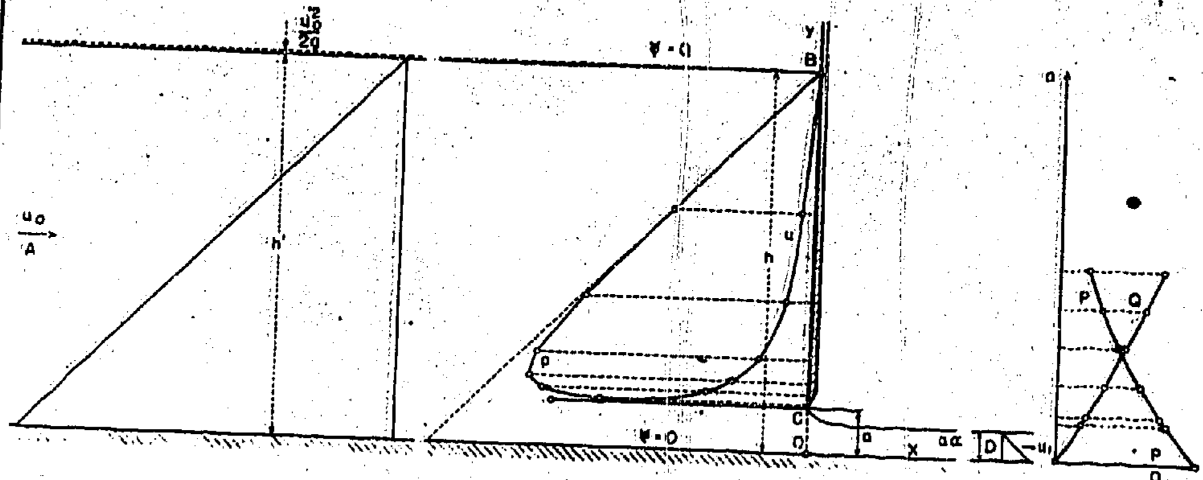

FIGURE 1

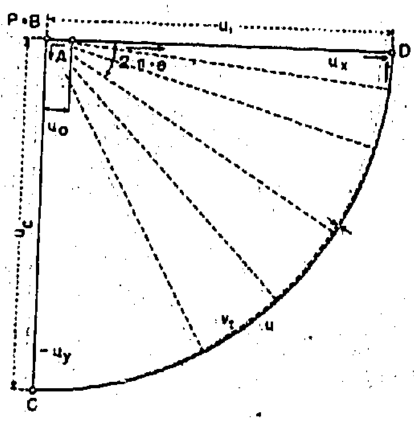

FIGURE 2

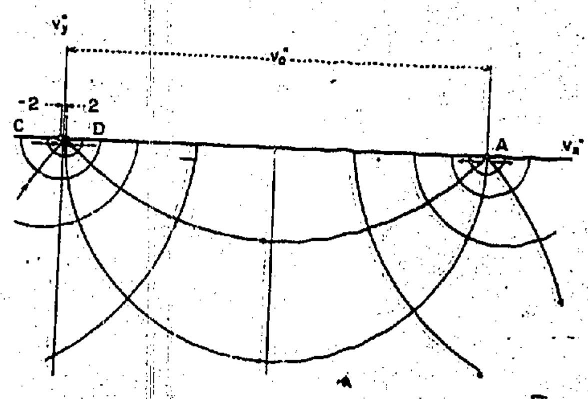

FIGURE 4

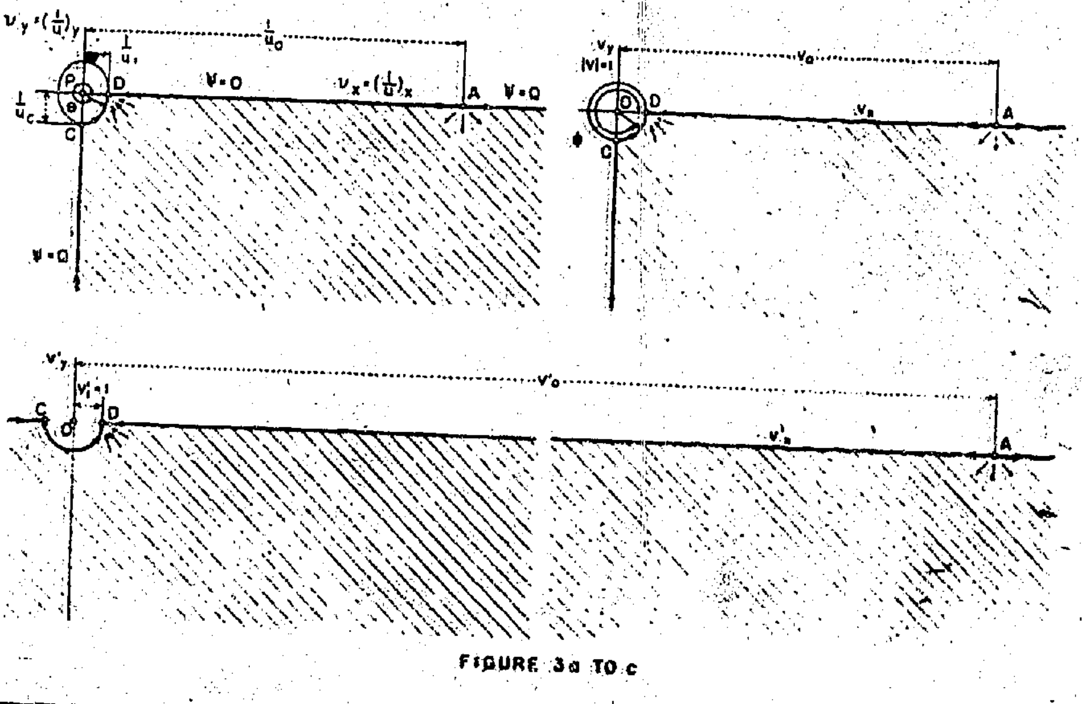

FIGURE 3a TO c